Hadronic light-by-light contribution to the muon $g-2$ from holographic QCD with solved $U(1)_A$ problem

Josef Leutgeb, Jonas Mager, and Anton Rebhan
Institut für Theoretische Physik, Technische Universität Wien, Wiedner Hauptstrasse 8-10, A-1040 Vienna, Austria

(Received 28 December 2022; accepted 20 February 2023; published 13 March 2023)

We employ the comparatively minimal extension of hard-wall AdS/QCD due to Katz and Schwartz which takes into account the $U(1)_A$ anomaly for computing hadronic light-by-light scattering contributions of pseudoscalar and axial-vector mesons to the anomalous magnetic moment of the muon a_μ. By including a gluon condensate as one extra tunable parameter besides those fixed by f_π and the pion, kaon, and rho masses, we obtain remarkably accurate fits for η and η' masses and their decay rates to photons, leading to a_μ contributions in complete agreement with the Standard Model result by the Muon $g-2$ Theory Initiative. Turning to the less well understood axial-vector contributions, we update our previous predictions obtained in flavor-symmetric hard-wall AdS/QCD models without $U(1)_A$ breaking.

DOI: 10.1103/PhysRevD.107.054021

I. INTRODUCTION

Since in 2021 the Muon $g-2$ Collaboration at Fermilab [1] has succeeded in confirming and improving the result of the E821/BNL measurement from 2006 [2] for the anomalous magnetic moment of the muon [3] and is under way on further increasing its accuracy, the existing uncertainties in the disagreeing theoretical Standard Model result [4] need to be scrutinized and also improved.

Whereas QED [5] and electroweak contributions [6,7] are sufficiently under control, the theoretical uncertainty is dominated by hadronic effects [8–31]. The largest contribution by far is the hadronic vacuum polarization (HVP), where a recent lattice calculation [32] is at variance with the result of the 2020 White Paper (WP) of the Muon $g-2$ Theory Initiative [4] beyond the respective estimated errors, leading to a less strong deviation from the experimental result if the lattice result is used in place of the data-driven one obtained in the WP. Once this discrepancy is resolved, it will be important to also reduce the uncertainty in the contribution from hadronic light-by-light scattering (HLBL), which at present has errors at the level of 20%, which in absolute numbers are comparable to the small errors aimed for in the case of HVP.

Besides the dominant pion-pole contribution to HLBL, which by now seems to be well understood, and where data-driven approaches and lattice evaluations agree perfectly, and the similarly well-determined contributions from η and η' mesons, other single-meson contributions are much less under control. An important contribution is expected in particular from axial-vector mesons, which like pseudoscalars have anomalous couplings to photons. However, theoretical predictions from various hadronic models vary a lot [3,8,12,33–35], which has led to a WP estimate of the axial-vector contribution with 100% uncertainty.

Holographic QCD models motivated by the AdS/CFT correspondence [36–38] have proved to be remarkably successful in qualitatively and also quantitatively describing hadronic observables, even those with a minimal set of parameters and the simplest geometry of anti–de Sitter space with a hard-wall (HW) cutoff. Such AdS/QCD models are not good enough to help with the current discrepancy between different predictions for the HVP contribution, where subpercent accuracy is required. However, they are certainly of interest for estimating the HLBL contributions.

In Ref. [39], we have revisited previous studies [40,41] of the pion-pole contribution to HLBL and its consequences for the value of $a_\mu = (g-2)_\mu/2$ using simple bottom-up AdS/QCD models in the chiral limit and we have found a satisfactory agreement with the data-driven and lattice approaches. The transition form factors obtained in AdS/QCD involve infinite towers of vector mesons, realizing vector meson dominance (VMD) in a form that is consistent with the asymptotic behavior derived from perturbative QCD [42] for both, the singly and the doubly virtual case.

In [43,44], also the contribution from the infinite tower of axial-vector mesons and their anomalous coupling to

photons has been calculated, and it could be shown that this takes care of the long-standing problem that simpler hadronic models had with the Melnikov-Vainshtein (MV) constraint [8] on the HLBL scattering amplitude (see [45] for a review assessing its impact on a_μ). In [46], we have more recently extended these calculations to include finite quark masses in the flavor-symmetric case. Besides demonstrating that the saturation of the MV constraint is entirely due to axial-vector mesons also away from the chiral limit, we have confirmed the relatively large contribution obtained in the chiral model.

In the present paper, we consider a minimal extension of the original hard-wall AdS/QCD model [47] due to Katz and Schwartz [48] for solving the $\mathrm{U}(1)_A$ problem associated with the relatively large η' mass. Going slightly beyond the setup of [48] by including a nonvanishing gluon condensate, we find that a very accurate match of the masses of η and η' mesons as well as their coupling strength to photons can be achieved. We then use this model to evaluate all contributions of pseudoscalar[1] and axial-vector-meson excitations, and thereby also the effect of the MV short-distance constraint, to the HLBL contribution to a_μ.

II. KATZ-SCHWARTZ MODEL: HARD-WALL AdS/QCD WITH SOLVED $U(1)_A$ PROBLEM

The model proposed by Katz and Schwartz [48,49] for solving the $U(1)_A$ problem builds upon the original HW AdS/QCD models of Refs. [47,50] which have turned out to provide a remarkably good approximation to the physics of light hadrons while introducing a minimal set of parameters.

In these models, one keeps the background geometry of pure anti–de Sitter space with metric

$$ds^2 = z^{-2}(\eta_{\mu\nu}dx^\mu dx^\nu - dz^2), \tag{1}$$

cut off by a hard wall at a finite value of the holographic radial coordinate at $z = z_0$ with suitable boundary conditions for the five-dimensional fields that at the conformal boundary at $z = 0$ represent sources for a set of QCD operators of interest. In addition to five-dimensional Yang-Mills fields $\mathcal{B}^{L,R}$ dual to left and right chiral-quark currents, a bifundamental scalar X representing quark-antiquark bilinears is introduced for spontaneous symmetry breaking of $U(N_f) \times U(N_f) \to U(N_f)_V$. Confinement is implemented by the cutoff at z_0, where boundary conditions for the five-dimensional fields are imposed.

[1]The pseudoscalar contributions to a_μ have been calculated before in [40] by Hong and Kim in the Katz-Schwartz model without gluon condensate. As discussed below, we disagree in the treatment of the Chern-Simons term.

The five-dimensional Yang-Mills action

$$S_{\mathrm{YM}} = -\frac{1}{4g_5^2}\int d^4x \int_0^{z_0} dz \sqrt{g} g^{PR} g^{QS} \times \mathrm{tr}(\mathcal{F}^{\mathrm{L}}_{PQ}\mathcal{F}^{\mathrm{L}}_{RS} + \mathcal{F}^{\mathrm{R}}_{PQ}\mathcal{F}^{\mathrm{R}}_{RS}), \tag{2}$$

where $P,Q,R,S = 0,\ldots,3,z$ and $\mathcal{F}_{MN} = \partial_M \mathcal{B}_N - \partial_N \mathcal{B}_M - i[\mathcal{B}_M, \mathcal{B}_N]$, is augmented by a Chern-Simons action $S_{\mathrm{CS}} = S^{\mathrm{L}}_{\mathrm{CS}} - S^{\mathrm{R}}_{\mathrm{CS}}$ to account for flavor anomalies, reading (in differential form notation)

$$S^{\mathrm{L,R}}_{\mathrm{CS}} = \frac{N_c}{24\pi^2}\int \mathrm{tr}\left(\mathcal{B}\mathcal{F}^2 - \frac{i}{2}\mathcal{B}^3\mathcal{F} - \frac{1}{10}\mathcal{B}^5\right)^{\mathrm{L,R}}, \tag{3}$$

(up to a boundary term at z_0 that needs to be subtracted [46,51]).

The bifundamental bulk scalar X is parametrized as [52]

$$X = e^{i\eta^a(x,z)t^a} X_0 e^{i\eta^a(x,z)t^a}, \tag{4}$$

where η^a, $a = 0,\ldots,8$, is a nonet of pseudoscalars excitations. The five-dimensional mass of X is fixed at[2] $M_X = -3$ by the scaling dimension of the dual operator $\bar{q}_L q_R$, leading to a vacuum solution

$$X_{0ij} = \frac{1}{2}m_{ij}z + \frac{1}{2}\sigma_{ij}z^3. \tag{5}$$

Choosing $N_f = 3$, we restrict ourselves to the isospin symmetric case $m_u = m_d = m_q \neq m_s$ with $X = \frac{1}{2}\mathrm{diag}(v_q, v_q, v_s)$.

For taking care of the $U(1)_A$ problem, a massless complex field Y is introduced, representing the gluon field strength squared $\alpha_s G^2_{\mu\nu}$ by its modulus and $\alpha_s G\tilde{G}$ by its phase, such that the Lagrangian of scalars reads

$$\mathcal{L}_{X,Y}/\sqrt{g} = \mathrm{tr}[|DX|^2 + 3|X|^2] + \frac{1}{2(\ln z\Lambda)^2}|DY|^2 + \frac{\kappa_0}{4}[\bar{Y}^{N_f}\det(X) + \mathrm{H.c.}], \tag{6}$$

where the logarithm in front of the kinetic term for Y accounts for the fact that its dual operators approach scaling dimension 4 only asymptotically. The complex scalar field Y is charged only under the singlet axial-vector field and hence its coupling is given by

$$D_M Y = \partial_M Y + \frac{i}{\sqrt{2N_f}}(\mathcal{B}^{L,0}_M - \mathcal{B}^{R,0}_M)Y. \tag{7}$$

Without the logarithm in (6), the field equations for Y would give a background $\langle Y\rangle = C + \Xi z^4$, where Ξ

[2]In [46] we have also studied the generalization to other values of M_X as proposed in [53].

represents a gluon condensate. After absorbing some numerical factors into C, the authors of [48] use the axial-anomaly relation and the QCD operator product expansion (OPE fit) of the flavor-singlet axial-vector correlation function to find

$$C = \frac{\alpha_s}{2\pi^2}\sqrt{2N_f}. \tag{8}$$

In QCD α_s is a running coupling and since in holography energy is identified with z^{-1}, they argue that α_s should be made z-dependent.

Matching $z\partial_z\alpha_s(z) \simeq -\beta_0\alpha_s^2$ with the one-loop QCD β function where $\beta_0 = 9/2\pi$ for $N_c = N_f = 3$ gives $\alpha_s^{-1} = \beta_0 \ln(\Lambda z)$, which is adopted for all $z < z_0 = \Lambda^{-1}$. Making α_s and therefore C depend on z is of course inconsistent with the equations of motion (without the logarithm), hence we use the modified version (6) including the logarithms. The presence of the logarithm in the action modifies the field equations for Y, leading to the general solution[3]

$$\langle Y\rangle = D_0 + D_1 z^4\left[(\ln z\Lambda)^2 - \frac{1}{2}\ln z\Lambda + \frac{1}{8}\right]. \tag{9}$$

For later convenience we define[4] $\tilde{Y}_0 = \frac{2}{\sqrt{2N_f}}(-\ln z\Lambda)^{-1}\langle Y\rangle$, which is parametrized as

$$\tilde{Y}_0 = \frac{C_0}{-\ln z\Lambda} - \Xi_0 z^4\left((\ln z\Lambda) - \frac{1}{2} + \frac{1}{8\ln z\Lambda}\right) \tag{10}$$

with $C_0 = \sqrt{2N_f}/(2\pi^2\beta_0) = \sqrt{2/3}/(3\pi)$. This background now naturally incorporates the running of α_s consistently and permits a nonvanishing gluon condensate through nonzero values of Ξ_0.

The coupling constant g_5 can be fixed by the OPE of the vector current correlator as

$$g_5^2 = 12\pi^2/N_c = (2\pi)^2 \quad \text{(OPE fit)}, \tag{11}$$

but we shall alternatively consider matching the decay constant of the ρ meson, which in the hard-wall model leads to [54]

$$g_5^2 = 0.894(2\pi^2) \quad (F_\rho\text{-fit}). \tag{12}$$

The latter leads to a significant improvement of the holographic result for the hadronic vacuum polarization: With the leading-order OPE fit (11), there is a deviation of 14% from $N_f = 2$ dispersive results, which is reduced to about 5% with (12) [54]. A reduction of g_5^2 by about 10% appears to be warranted also by comparing with next-to-leading order QCD results for the vector correlator at moderately large Q^2 values [55–57]. It also brings our $N_f = 2$ results for the pion-pole contribution to a_μ [46] in line with the WP result.

With g_5 and C_0 fixed by the UV behavior, the free parameters of the model are (i) the location of the hard wall, z_0, which can be identified with Λ^{-1}, and will be set by the ρ meson mass, (ii) quark masses in $m_{ij} = \mathrm{diag}(m_q, m_q, m_s)$, (iii) chiral condensates σ_{ij}, which we shall assume to be given by a single parameter, $\sigma_{ij} = \sigma\delta_{ij}$, and (iv) Ξ_0, which corresponds to the gluon condensate $\alpha_s\langle G^2\rangle$. The coupling constant κ_0, on the other hand, can be set to some sufficiently large value, since it turns out that for $\kappa_0 \gg 1$ all results depend only weakly on κ_0 [48].

III. MESON MODES AND TRANSITION FORM FACTORS

Vector-meson dominance is naturally part of this model by relating a nonzero boundary value $\mathcal{B}_\mu^V(0) = e\mathcal{Q}A_\mu^{\text{e.m.}}$ to the background electromagnetic potential and setting $\mathcal{Q} = \mathrm{diag}(\frac{2}{3}, -\frac{1}{3}, -\frac{1}{3})$ according to the charges of up, down, and strange quarks. Normalizable modes of $\mathcal{B}_V$ and $\mathcal{B}_A$ correspond to vector and axial-vector mesons, the longitudinal polarizations of the latter mixing with the pseudoscalars η^a in X. Ignoring scalar excitations, which in this model do not couple to photons,[5] the additional Y field also involves a pseudoscalar a through its phase

$$Y = \langle Y\rangle \exp[i2a(x,z)/\sqrt{2N_f}], \tag{13}$$

which corresponds to a pseudoscalar glueball in the boundary theory (G) that couples to photons via its mixing with the flavor-singlet pseudoscalar mesons.

To determine the pseudoscalar eigenmodes in the mixed $a = (0,8)$-sector, we consider the equations of motion[6]

$$\partial_z\left(\frac{1}{z}\partial_z\varphi_n^a\right) + g_5^2\frac{M_{ab}^2}{z^3}(\eta_n^b - \varphi_n^b) + \delta^{a0}g_5^2\frac{\tilde{Y}_0^2}{z^3}(a_n - \varphi_n^0) = 0, \tag{14}$$

$$\partial_z\left(\frac{\tilde{Y}_0^2}{z^3}\partial_z a_n\right) + m_n^2\frac{\tilde{Y}_0^2}{z^3}(a_n - \varphi_n^0) + \kappa N_f\frac{v_q^2 v_s}{z^5}\left(\frac{\tilde{Y}_{00}}{4}\right)^{N_f}(\eta_n^0 - a_n) = 0, \tag{15}$$

[3]Here we also deviate from Ref. [48], where a gluon condensate, here parametrized by D_1 was neglected and only C of the background solution had to be modified.

[4]This is the same redefinition that [48] use, except for the logarithm.

[5]See Ref. [58] for extensions of the HW model where further interactions are switched on to have scalars couple to photons in order to study their potential contribution to a_μ in AdS/QCD.

[6]We assume a summation over $a = (0,8)$ for contracted flavor indices and work in the $A_z = 0$ gauge.

$$\frac{m_n^2}{g_5^2}\frac{1}{z}\partial_z\varphi_n^a - \delta^{a0}\frac{\tilde{Y}_0^2}{z^3}\partial_z a_n - \frac{M_{ab}^2}{z^3}\partial_z\eta_n^b = 0, \tag{16}$$

with the longitudinal component of the axial gauge field $\partial_\mu\varphi^a = A_\mu^{a\|}$ and an effective 5-dimensional mass term

$$M_{ab}^2 = \frac{1}{3}\begin{pmatrix} 2v_q^2 + v_s^2 & \sqrt{2}(v_q^2 - v_s^2) \\ \sqrt{2}(v_q^2 - v_s^2) & v_q^2 + 2v_s^2 \end{pmatrix}, \tag{17}$$

with $v_{q,s} = m_{q,s}z + \sigma z^3$. Here we have also absorbed numerical constants in κ_0 and renamed it to κ, and we defined $\tilde{Y}_{00} = -\tilde{Y}_0 \ln z\Lambda/C_0$.

The fields φ^a are dual to QCD operators $-\partial_\mu J_A^{\mu,a}$, and the glueball field a is dual to $-\sqrt{2N_f}K$, where K is the instanton density $K = \frac{\alpha_s}{8\pi}G^a_{\mu\nu}\tilde{G}^{a\mu\nu}$. This new field a allows then among other things to compute overlaps of the instanton density K with pseudoscalar modes $\eta, \eta', \ldots$ and the topological susceptibility.

All fields of the normalizable modes have Dirichlet boundary conditions in the UV at $z = 0$, Neumann boundary conditions in the IR at $z = z_0$, and are canonically normalized by

$$\int dz\left(\frac{M_{ab}}{z^3}(\eta_n^a(\eta_m^b - \varphi_m^b)) + \frac{\tilde{Y}_0{}^2}{z^3}a_n(a_m - \varphi_m^0)\right) = \delta_{nm}. \tag{18}$$

From the Chern-Simons term (3) we obtain the transition form factor (TFF)

$$F_n(Q_1^2, Q_2^2) = \mathrm{tr}(t^a\mathcal{Q}^2)F_n^a(Q_1^2, Q_2^2), \tag{19}$$

with [46]

$$F_n^a(Q_1^2, Q_2^2) = -\frac{N_c}{2\pi^2}\left(\int dz\varphi_n'^a(z)\mathcal{J}(Q_1, z)\mathcal{J}(Q_2, z) - [\varphi_n^a(z) - \eta_n^a(z)]\mathcal{J}(Q_1, z)\mathcal{J}(Q_2, z)|_{z_0}\right), \tag{20}$$

where the vector bulk-to-boundary propagator

$$\mathcal{J}(Q, z) = Qz\left[K_1(Qz) + \frac{K_0(Qz_0)}{I_0(Qz_0)}I_1(Qz)\right] \tag{21}$$

describes virtual photons with spacelike momentum $q^2 = -Q^2$.

Note that (20) involves the subtraction of a boundary term at $z = z_0$, which is absent in [48], but (20) also differs from the corresponding expression given in [51], where $(\varphi_n^a - \eta_n^a)'$ appears in the integral. As discussed in [46], this is only correct in the chiral limit and for the ground-state pion, but not in the massive case. Our results for the pseudoscalar TFFs therefore also differ from Ref. [40], where the TFFs for ground-state pseudoscalars in the Katz-Schwartz model have been evaluated with the inapplicable chiral formula of [51].

We can also generalize the asymptotic results and the sum relations obtained in [46] in the nonchiral but flavor-symmetric case to the asymmetric case $m_s \neq m_q$ with broken $\mathrm{U}(1)_A$ symmetry. Most importantly, we can derive the anomaly equations

$$\sum_n f_n^a F_n^a(0,0) = \frac{N_c}{2\pi^2}, \quad a = 0, 3, \text{ or } 8 \text{ (fixed)}, \tag{22}$$

and the short-distance constraint (SDC)

$$F_n^a(Q^2(1+w), Q^2(1-w)) \to \frac{N_c}{2\pi^2}g_5^2 f_n^a\frac{1}{Q^2}f(w) \tag{23}$$

for $Q \to \infty$ with the asymmetry function

$$f(w) = \frac{1}{w^2} - \frac{1-w^2}{2w^3}\ln\frac{1+w}{1-w}, \tag{24}$$

and the pseudoscalar decay constants

$$f_n^a = -g_5^{-2}\partial_z\varphi_n^a/z|_{z\to 0}. \tag{25}$$

Note that the decay rate associated with the glueball field,

$$f_G^n = \tilde{Y}_0^2\partial_z a_n/z^3|_{z\to 0} \tag{26}$$

does not contribute to the TFF. In QCD f_G^n computes $(-\sqrt{2N_f})\langle\Omega|K|P_n\rangle$, where P_n is the respective pseudoscalar particle.

As far as we know, the sum rules (22) have not appeared in the literature before in this general form where they include mixing due to finite quark masses $m_s \neq m_q$ and breaking of the $\mathrm{U}(1)_A$ symmetry at finite N_c. They involve the components F_n^a of the TFFs F_n defined by (19), which at least in lattice QCD could be determined directly by varying the quark-charge matrix $\mathcal{Q}$.

In general, all modes contribute to (22). In the limit of vanishing quark masses, one has $m_n^2 f_n^{3,8} = O(m_q)$ for each n (as discussed in the Appendix of [46] in the holographic setup). This implies that for $a = 3$ and 8 only the massless Goldstone bosons contribute to the sum rules, whereas excited pseudoscalar modes decouple from the anomaly relations, while they can still have nonzero $F_n(0,0)$. In the $a = 0$ sector, we instead find $f_n^0 m_n^2 + f_G^n = O(m_q)$, and the mass of the η' meson is nonzero (in the chiral limit between 600 MeV and 700 MeV, depending on the precise value of Ξ_0). This means that even in the chiral limit (22) receives contributions from all higher modes in the $a = 0$ sector, which is qualitatively different from the $a = 3$, 8 sectors.

Comparing the axial-vector sector to [46], the $a = 3$ sector is unmodified, but the $a = (0, 8)$ equations of motion are changed to

$$\partial_z\left(\frac{1}{z}\partial_z\psi^a_{A,n}(z)\right) + \frac{1}{z}m^2_{A,n}\psi^a_{A,n}(z) - \frac{g_5^2(M^2_{ab} + \delta_{0a}\delta_{0b}\tilde{Y}_0^2)}{z^3}\psi^b_{A,n}(z) = 0. \tag{27}$$

In each case the axial-vector TFF is given by[7]

$$A_n(Q_1^2, Q_2^2) = \mathrm{tr}(t^a\mathcal{Q}^2)A^a_n(Q_1^2, Q_2^2), \tag{28}$$

with

$$A^a_n(Q_1^2, Q_2^2) = \frac{2g_5}{Q_1^2}\int_0^{z_0} dz\left[\frac{d}{dz}\mathcal{J}(Q_1, z)\right]\mathcal{J}(Q_2, z)\psi_n^{A,a}(z). \tag{29}$$

At large Q^2 we obtain as in [43,46]

$$A^a_n(Q^2(1+w), Q^2(1-w)) \to \frac{g_5^2F^a_{A,n}}{Q^4}f_A(w), \tag{30}$$

with the decay constants

$$F^a_n = -g_5^{-2}\partial_z\psi^a_{A,n}/z|_{z\to 0} \tag{31}$$

and the asymmetry function

$$f_A(w) = \frac{1}{w^4}\left[w(3-2w) + \frac{1}{2}(w+3)(1-w)\ln\frac{1-w}{1+w}\right], \tag{32}$$

in agreement with the asymptotic form derived from QCD in [42].

At $Q_1^2 = Q_2^2 = 0$, the axial-vector TFF in (28) is related to the form factor $F^{(1)}_{\mathcal{A}_n\gamma^*\gamma^*}(0,0)$ defined in [59] via $m_{A_n}^{-2}F^{(1)}_{\mathcal{A}_n\gamma^*\gamma^*}(0,0) = \frac{N_c}{4\pi^2}A_n(0,0)$. (See the Appendix of [43] for more details.)

The most general expression for axial-vector amplitudes has actually one further asymmetric structure function [34,59,60], which is set to zero in the holographic model and whose phenomenological importance has not yet been established; see Ref. [60] for a compilation of the available phenomenological information.

[7]Note that in the flavor-symmetric case considered in [43] A without flavor index was defined differently, corresponding to (the then a-independent) A^a here.

IV. RESULTS

A. Parameter settings

As one of the input data which we fit, we take the ρ meson mass[8] $m_\rho = \gamma_{0,1}z_0^{-1} = 2.40483\ldots z_0^{-1}$, where $\gamma_{0,1}$ is the first zero of the Bessel function J_0. Following Ref. [52], we have chosen $z_0^{-1} = 0.3225$ GeV corresponding to $m_\rho = 775.556$ MeV. This fixes the location of the hard wall, z_0, and Λ in the expression for α_s. The coupling g_5 is either set by the leading-order OPE result (11) or the slightly reduced value (12) obtained by fitting the ρ meson decay constant, where the TFFs reach only 89.4% of the OPE and Brodsky-Lepage limits, thereby coming closer to next-to-leading order results at moderately large, experimentally relevant energy scales.

The isospin-symmetric quark-mass parameter m_q and the chiral-condensate parameter σ are chosen such that $m_\pi = 134.97$ MeV and $f_\pi = 92.21$ MeV [61]; the strange quark mass parameter m_s is chosen such that [62]

$$m_K^2 = \frac{1}{2}(m^2_{K_\pm} + m^2_{K_0}) - \frac{1}{2}(m^2_{\pi_\pm} - m^2_{\pi_0}) = (495.007\ \mathrm{MeV})^2 \tag{33}$$

in order to minimize isospin-breaking contributions.

For the two choices of g_5, we consider the model with and without a gluon condensate parameter Ξ_0. When $\Xi_0 = 0$ (referred to as model version v0 in the following), we obtain predictions for m_η and m'_η that are around 10% lower than the real-world values, in accordance with Ref. [48] who had omitted to turn on a nonzero Ξ_0. Fitting Ξ_0 such that $(1 - m_\eta^{\mathrm{th}}/m_\eta^{\mathrm{exp}})^2 + (1 - m_{\eta'}^{\mathrm{th}}/m_{\eta'}^{\mathrm{exp}})^2$ is minimized (model v1), m_η and m'_η can be matched at the percent level, as shown in Table II. In the four versions of our model, we have chosen a large value of $\kappa = 700$, in order to be in the regime where the dependence on κ is rather weak.

B. Decay constants and photon coupling

Up to the slightly different choice of f_π, the results for the mesons in the isotriplet sector, where Ξ_0 does not play a role, are identical to the HW1m model presented in [46] for $g_5 = 2\pi$. Table I generalizes this to the case where g_5 is fitted to match F_ρ.

In Tables II and III, detailed results for the two versions v0 and v1 are given for the first few pseudoscalar and axial-vector modes in the isosinglet sector, showing their mixing behavior in the decay constants f^8, f^0, f_G for the η's, and F_A^8, F_A^0 for the f_1's, as well as in the coupling to real

[8]A shortcoming of the minimal HW models considered here is that the strange quark mass modifies the vector meson masses too little compared to reality: ρ, ω, and ϕ mesons are degenerate, the mass of K^* is raised to only 0.79 GeV.

TABLE I. Results for pseudoscalar and axial-vector mesons in the isotriplet sector (the gluon condensate parameter Ξ_0 does not play a role here). All quantities in units of (powers of) GeV; values marked with a star (⋆) are input data.

	$g_5^2=(2\pi)^2$							$g_5^2=0.894(2\pi)^2$						
	π^0	π^*	a_1	a_1^*	a_1^{**}	a_1^{***}	a_1^{****}	π^0	π^*	a_1	a_1^*	a_1^{**}	a_1^{***}	a_1^{****}
m	0.135⋆	1.891	1.363	2.137	2.987	3.935	4.916	0.135⋆	1.841	1.278	2.047	2.936	3.902	4.891
$f\vee F_A/m_A$	0.09221⋆	0.00157	0.175	0.204	0.263	0.311	0.330	0.09221⋆	0.00173	0.173	0.217	0.280	0.329	0.330
$F(0,0)\vee A^3(0,0)$	0.277	−0.203	20.96	3.31	−0.336	2.16	0.370	0.276	−0.199	19.46	4.87	−0.413	2.05	0.325
$a_\mu\times10^{11}$	66.1	0.73	7.83	1.24	0.44	0.28	0.11	63.4	0.71	7.09	1.47	0.42	0.26	0.10

photons given by $F(0,0)$ and $A(0,0)$, respectively. All results are given in units of GeV raised to the appropriate power; note that the mass dimension of f^8 and f^0 is 1, but that of f_G is 3; $F(0,0)$ and $A(0,0)$ have mass dimensions -1 and -2, respectively.

Mixing is in fact energy dependent in the holographic model because the components of the holographic wave functions depend nontrivially on the holographic coordinate z which corresponds to inverse energy. The mixing angles read from decay constants thus differ from those read from the components of the photon coupling. Moreover, the pseudoscalar mixings are different when determined from η or η' (and similarly in the case of f_1 and f_1'). Indeed, a phenomenological need for an energy-dependent mixing in the case of η and η' has been argued for in [63,64].

The pseudoscalars η, η' and a third ground-state η'' meson arise from mixing of flavor-octet and flavor-singlet degrees of freedom with the pseudoscalar glueball G, each followed by an infinite tower of excited states. The ground state modes are dominantly flavor octet, singlet, and glueball judging from

TABLE II. Results for the isoscalar pseudoscalar sector, for the model with (v1) and without (v0) gluon condensate, and for two choices of g_5: $g_5=2\pi$ corresponding to matching the vector correlator to the leading-order UV-behavior in QCD, and the reduced value corresponding to a fit of F_ρ. All dimensionful quantities in units of (powers of) GeV.

	$\Xi_0=0$						$\Xi_0=0$					
	$g_5^2=(2\pi)^2$						$g_5^2=0.894(2\pi)^2$					
(v0)	η	η'	G/η''	$\eta^{(3)}$	$\eta^{(4)}$	$\eta^{(5)}$	η	η'	G/η''	$\eta^{(3)}$	$\eta^{(4)}$	$\eta^{(5)}$
m	0.513	0.840	1.862	1.999	2.257	2.705	0.503	0.819	1.764	1.948	2.207	2.638
$m-m^{\rm exp}$	−6.4%	−12.3%					−8.2%	−14.5%				
f^8	0.0917	−0.0565	0.00197	0.0266	0.0121	0.0080	0.0902	−0.0624	0.00405	0.0293	0.0132	0.00837
f^0	0.0394	0.0945	−0.0212	−0.00823	−0.0390	0.0362	0.0446	0.0952	−0.0224	−0.00802	−0.0416	0.0337
f_G	−0.0264	−0.0385	0.0674	−0.0400	0.154	−0.310	−0.0265	−0.0344	0.0600	−0.0454	0.156	−0.280
$F^8(0,0)$	1.46	−0.674	0.177	−1.18	0.00233	0.236	1.41	−0.737	0.0640	−1.16	0.0239	0.241
$F^0(0,0)$	0.776	1.42	0.169	0.0383	1.08	0.229	0.828	1.34	0.00310	0.00492	1.10	0.253
$F(0,0)$	0.351	0.322	0.0629	−0.103	0.293	0.0851	0.361	0.295	0.00700	−0.110	0.302	0.0922
$F-F^{\rm exp}$	+28(2)%	−6(2)%					+32(2)%	−14(2)%				
$a_\mu\times10^{11}$	32.8	15.7	0.055	0.14	0.79	0.16	34.0	13.3	0.003	0.16	0.85	0.16

	$\Xi_0=0.01051$						$\Xi_0=0.01416$					
	$g_5^2=(2\pi)^2$						$g_5^2=0.894(2\pi)^2$					
(v1)	η	η'	G/η''	$\eta^{(3)}$	$\eta^{(4)}$	$\eta^{(5)}$	η	η'	G/η''	$\eta^{(3)}$	$\eta^{(4)}$	$\eta^{(5)}$
m	0.557	0.950	1.992	2.390	2.954	3.214	0.561	0.947	1.943	2.428	2.914	3.317
$m-m^{\rm exp}$	+1.7%	−0.8%					+2.4%	−1.1%				
f^8	0.101	−0.0385	−0.0267	0.0116	−0.0228	−0.0049	0.103	−0.0393	−0.0299	0.0112	−0.0253	−0.00767
f^0	0.0272	0.113	0.0049	−0.0492	−0.00115	−0.0214	0.0298	0.121	0.00761	−0.0522	0.00320	−0.0128
f_G	−0.0298	−0.0774	0.053	0.233	0.1483	0.269	−0.0313	−0.0821	0.048	0.260	0.1236	0.214
$F^8(0,0)$	1.55	−0.431	1.19	−0.0478	−0.887	0.167	1.53	−0.442	1.149	−0.0312	−0.877	0.129
$F^0(0,0)$	0.468	1.40	0.0051	0.904	0.0300	0.0867	0.444	1.31	−0.000026	0.837	0.0307	0.130
$F(0,0)$	0.276	0.340	0.116	0.241	−0.0772	0.0397	0.268	0.313	0.111	0.225	−0.0760	0.0477
$F-F^{\rm exp}$	+1(2)%	−0(2)%					+2(2)%	−8(2)%				
$a_\mu\times10^{11}$	19.3	16.9	0.19	0.53	0.043	0.008	17.6	14.9	0.18	0.45	0.039	0.007

the corresponding decay constants evaluated at $z \to 0$, while the first excited triplet $\eta^{(3)}$ to $\eta^{(5)}$ shows a more involved mixing behavior. The decay constants for η and η' agree reasonably well with the recent lattice results of Ref. [65], where also pseudoscalar matrix elements have been evaluated. Our results for f_G correspond to $\sqrt{N_f/2}a$ in [65] and also agree reasonably well. The ratio $a_{\eta'}/a_\eta$ is between 2 and 2.5 depending on the renormalization scale. This is better in line with our model v1 that includes a nonzero gluon condensate, where $f_{G,\eta'}/f_{G,\eta} = 2.60$ and 2.66 for the two choices of g_5, while model v0 has 1.46 and 1.30.

Without gluon condensate (v0), the results for $F(0,0)$ show rather poor agreement with experimental results for the η meson with deviations of around 30%, while those for $F_{\eta'\to\gamma\gamma}(0,0)$ are much better. With gluon condensate (model v1), where the masses of η and η' agree with experimental data at the percent level, both couplings turn out to agree remarkably well with the experimental values.

For isosinglet axial-vector mesons (Table III), both model versions predict generally too high values of f_1 and f_1' masses (+8% to +28% compared to PDG data [66]). The f_1 and f_1' mesons are obtained as dominantly flavor octet and flavor singlet, respectively. In the holographic model, the mixing angle is an energy or z dependent quantity. In the case of the f_1 mesons, it is usually extracted from equivalent photon decay rates at zero virtuality, where the experimental results from the L3 experiment read [67,68]

$$\tilde{\Gamma}_{\gamma\gamma} = \begin{cases} 3.5(8)\ \text{keV} & \text{for } f_1 = f_1(1285) \\ 3.2(9)\ \text{keV} & \text{for } f_1' = f_1(1420) \end{cases}. \tag{34}$$

With the definition

$$f_1 = \cos\theta_A f^0 + \sin\theta_A f^8 \tag{35}$$

and the assumption that $\tilde{\Gamma}_{\gamma\gamma} \propto m_A$, one has

$$\tan^2\left(\theta_A - \arcsin\frac{1}{3}\right) = \frac{m_{f_1}\tilde{\Gamma}_{\gamma\gamma}^{f_1'}}{m_{f_1'}\tilde{\Gamma}_{\gamma\gamma}^{f_1}}, \tag{36}$$

leading to [42] $\theta_A = 62(5)°$, superficially agreeing with model version v0. However, in the holographic model we have

$$\tilde{\Gamma}_{n,\gamma\gamma} = \frac{\pi\alpha^2 m_A}{12}\left[\frac{N_c m_A^2}{4\pi^2}A_n(0,0)\right]^2 \sim m_A(m_A/\Lambda)^4, \tag{37}$$

resulting in $\theta_A = 56(5)°$ for the experimental value, which does not fit to the results for either v0 or v1, the latter disagreeing even more than the former.[9] While the mixing angle depends rather strongly on Ξ_0, the combination $\sqrt{[A^8(0,0)]^2 + [A^0(0,0)]^2}$ changes only slightly between models v0 and v1, and it is also close to the value of $A(0,0)$ in the isotriplet sector, as well as to the same quantity in the chiral hard-wall model [43], $(21.04\ \text{GeV})^{-2}$. Matching

TABLE III. Results for the isoscalar axial-vector sector, for the model with (v1) and without (v0) gluon condensate, and the two choices g_5 (OPE fit) and g_5 (F_ρ-fit). Here $\theta_A \equiv \arctan(A^8(0,0)/A^0(0,0))$ for both f_1 and f_1', and $A(0,0) = \mathrm{tr}(t^a\mathcal{Q}^2)A^a(0,0) = [A^8(0,0) + \sqrt{8}A^0(0,0)]/6\sqrt{3}$. All dimensionful quantities are given in units of (powers of) GeV. In the a_μ contributions, about 58% are due to the longitudinal part of the axial-vector-meson propagator, which contributes to the MV constraint.

	$\Xi_0 = 0$		$\Xi_0 = 0$	
	$g_5^2 = (2\pi)^2$		$g_5^2 = 0.894(2\pi)^2$	
(v0)	f_1	f_1'	f_1	f_1'
m	1.460	1.651	1.388	1.598
$m - m^{\text{exp}}$	+14%	+16%	+8%	+12%
F_A^8/m	0.163	−0.0732	0.165	−0.0627
F_A^0/m	0.0743	0.169	0.0690	0.180
$A^8(0,0)$	19.27	−8.649	18.38	−7.194
$A^0(0,0)$	8.676	19.21	7.310	18.62
θ_A	65.8°	−24.2°	68.3°	−21.1°
$A(0,0)$	4.22	4.40	3.76	4.37
m^*	2.241	2.614	2.147	2.561
m^{**}	3.056	3.580	2.999	3.535
$a_\mu \times 10^{11}$	11.0	10.8	9.08	11.0
$a_\mu^* \times 10^{11}$	0.61	1.50	0.62	1.54
$a_\mu^{**} \times 10^{11}$	0.18	1.08	0.16	0.99
$a_\mu^{***} \times 10^{11}$	0.09	0.42	0.08	0.39
$a_\mu^{****} \times 10^{11}$	0.04	0.27	0.03	0.25

	$\Xi_0 = 0.01051$		$\Xi_0 = 0.01416$	
	$g_5^2 = (2\pi)^2$		$g_5^2 = 0.894(2\pi)^2$	
(v1)	f_1	f_1'	f_1	f_1'
m	1.481	1.810	1.410	1.820
$m - m^{\text{exp}}$	+15%	+27%	+10%	+28%
F_A^8/m_A	0.176	−0.0299	0.176	−0.0167
F_A^0/m_A	0.0365	0.201	0.0292	0.219
$A^8(0,0)$	20.77	−3.842	19.58	−2.556
$A^0(0,0)$	3.857	20.07	2.690	19.00
θ_A	79.5°	−10.8°	82.2°	−7.7°
$A(0,0)$	3.05	5.09	2.62	4.93
m^*	2.246	2.862	2.153	2.891
m^{**}	3.058	3.869	3.004	3.907
$a_\mu \times 10^{11}$	5.71	14.3	4.34	13.6
$a_\mu^* \times 10^{11}$	0.36	1.01	0.33	0.91
$a_\mu^{**} \times 10^{11}$	0.11	1.11	0.05	0.99
$a_\mu^{***} \times 10^{11}$	0.01	0.33	0.02	0.24
$a_\mu^{****} \times 10^{11}$	0.01	0.28	0.05	0.15

[9]It would be interesting to revisit this issue in other holographic QCD models, in particular ones that are closer to a string-theoretic top-down construction such as the models of Refs. [69–71].

$A(0,0)$ with $\tilde{\Gamma}_{\gamma\gamma} \propto m_A(m_A/\Lambda)^4$ to the L3 results leads to a value of 15.2(2.0) GeV^{-2} so that the holographic results, which read 20–21 GeV^{-2} when $g_5 = 2\pi$ and 19–20 GeV^{-2} for the reduced g_5, are somewhat too high for f_1 and f_1', but not excluded for a_1, for which Ref. [34] has a concordant estimate of 19.3 (5.0) GeV^{-2}.

C. Transition form factors

For the HLBL contribution of single mesons to a_μ, their singly- and doubly-virtual TFFs are of critical importance.

As in the chiral HW model [39], we find excellent agreement of the singly virtual result for the pion TFF with available experimental data, see Fig. 1. At virtualities relevant for a_μ, the results with g_5 fitted to F_ρ, where the asymptotic limit is 89.4% of the Brodsky-Lepage value, seem to give the best match.

For the symmetric doubly virtual TFF the comparison is made with the dispersive result of Ref. [21] and the lattice result of Ref. [22] in Fig. 2. Both choices of g_5 are within the error band of the dispersive result, while the result for the reduced g_5 is also within the error band of the lattice result and moreover happens to coincide with the central values of the dispersive approach within line thickness of the plot throughout the entire range of Q^2.

With η and η' mesons, there is a rather strong dependence on the parameter Ξ_0 representing a gluon condensate. With this parameter turned on, the masses of η and η' can be matched to percent level accuracy, and the resulting prediction for $F_{P\gamma\gamma}(0,0)$ is then in complete agreement with experiment for $g_5 = 2\pi$ (see Table II), while with reduced g_5 this value is slightly underestimated in the case of η'. For the singly virtual TFF of η, only the results with nonzero Ξ_0 are close to the experimental data, see Fig. 3. They match those at low Q^2 quite well, but are generally larger at higher virtualities. In the case of η', all model versions agree with the low-Q^2 date due to L3, while at higher Q^2 the results without gluon condensate agree with more of the data points, but only with unreduced $g_5 = 2\pi$.

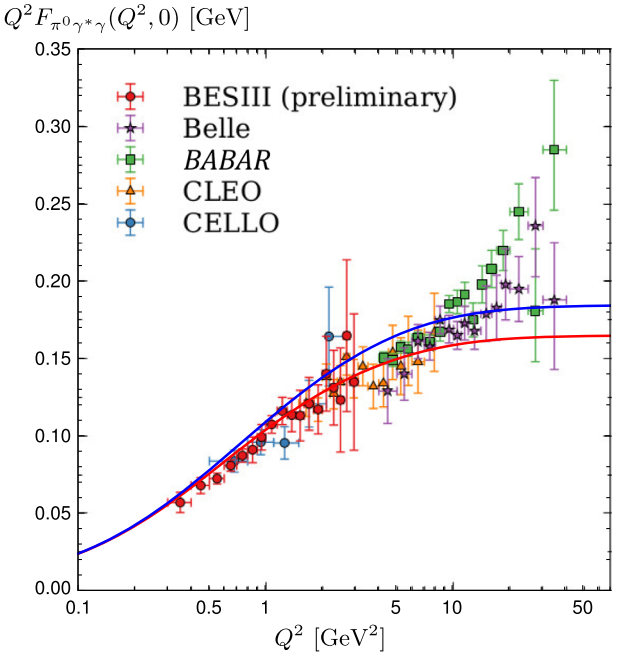

FIG. 1. Holographic results for the single virtual TFF $Q^2F(Q^2,0)$ for π^0, plotted on top of experimental data as compiled in Fig. 53 of Ref. [4] for $g_5 = 2\pi$ (OPE fit, blue) and the reduced value (red) corresponding to a fit of F_ρ. (For π^0 results for the model with and without gluon condensate coincide.)

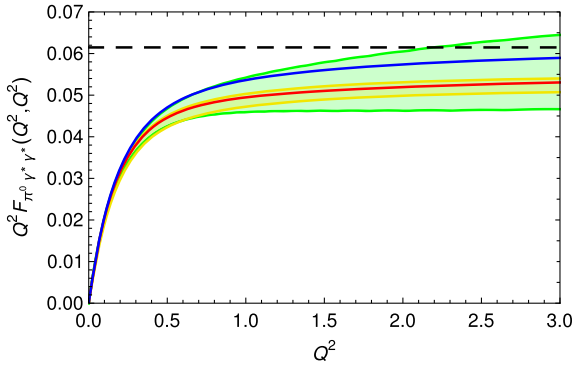

FIG. 2. Holographic results for the doubly virtual $F_{\pi^0\gamma^*\gamma^*}$ compared to the dispersive result of Ref. [21] (green band) and the lattice result of Ref. [22] (yellow band); the OPE limit given by the dashed horizontal line. The upper full line (blue) corresponds to $g_5 = 2\pi$ (OPE fit), the lower (red) one to the reduced value g_5 (F_ρ-fit). (Here the two versions with and without gluon condensate coincide.)

In contrast to the case of π^0, there are also several experimental data points for the doubly virtual TFF of η'. As opposed to the simple VMD model considered in [72] and represented by the cyan circles in Fig. 4, the holographic results are within 1 and 2 standard deviations. For the lowest virtualities $Q_1^2 = Q_2^2 = 6.48$ GeV^2, which are the most significant for a_μ, all versions of the model come close to the experimental result. With gluon condensate, the agreement is better with the reduced g_5, whereas without gluon condensate, a reduction of g_5 to fit F_ρ moves the prediction slightly outside the error bar.

All in all, the model with gluon condensate and reduced g_5 seems to be the optimal choice regarding pseudoscalar TFFs.

D. HLBL contribution to a_μ

Tables I and II include also the individual contributions of the listed pseudoscalar and axial-vector meson modes to a_μ, which are collected in Table IV for the model with nonzero gluon condensate (v1) with $g_5 = 2\pi$ (OPE-fit) and the reduced value (12) from fitting the ρ meson decay. Only with the extra parameter Ξ_0 for the gluon condensate, the predictions for $F_{P\gamma\gamma}(0,0)$ and masses of η and η' match experimental data with good accuracy. With reduced g_5

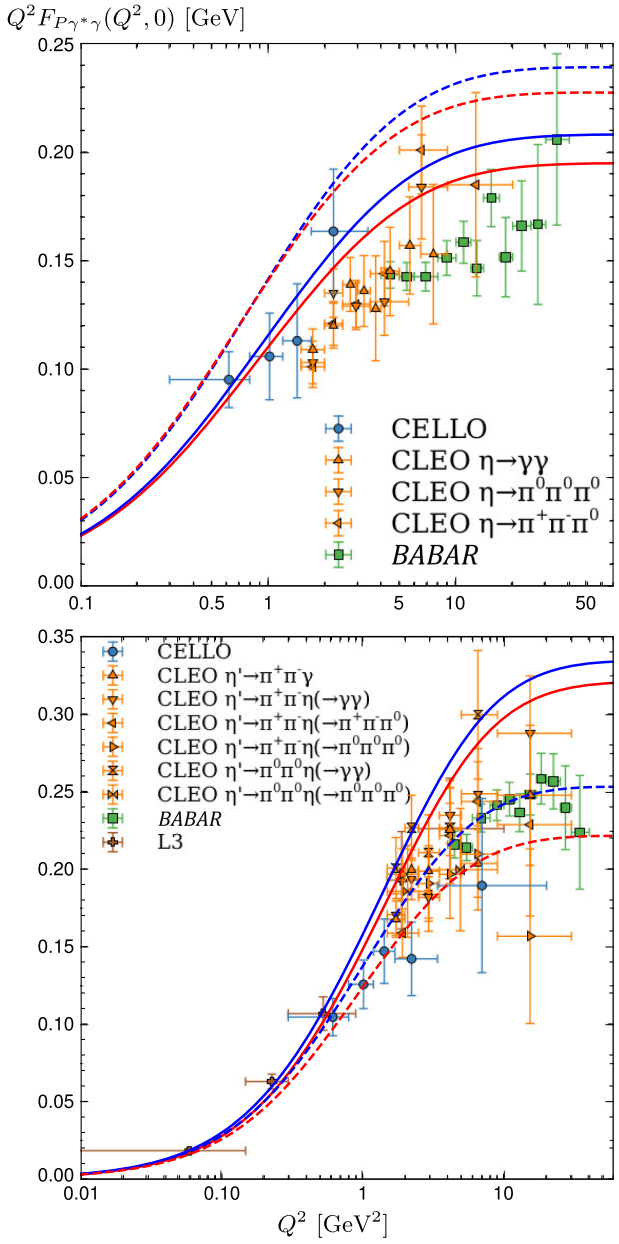

FIG. 3. Holographic results for the single virtual TFF $Q^2F(Q^2,0)$ for η and η' plotted on top of experimental data as compiled in Fig. 54 of Ref. [4] for $g_5 = 2\pi$ (OPE fit, blue) and the reduced value (red) corresponding to a fit of F_ρ. Full lines are with gluon condensate (version v1), dashed lines without (v0).

(F_ρ-fit), the predictions for $a_\mu^{\pi^0}$ and $a_\mu^{\eta'}$ are extremely close to the central values adopted by the White Paper [4], and those for η agree within 1σ.

The holographic model also includes a third ground-state η meson, which we called η'', the result of mixing with the pseudoscalar glueball G. It contributes only 0.2×10^{-11}, but there is also a whole tower of excited η modes, which together with excited pion modes contribute around 1.5×10^{-11} so that the total pseudoscalar poles prediction for model v1 (F_ρ-fit) is close to the upper end of the

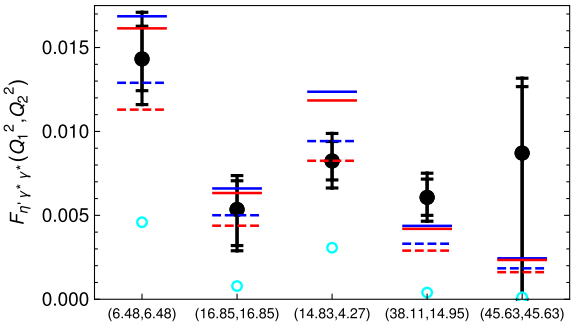

FIG. 4. Holographic results for the doubly virtual $F_{\eta'\gamma^*\gamma^*}$ compared to *BABAR* data points (black) and a simple VMD model fitted with singly virtual data (cyan circles) [72]. Full lines are with gluon condensate (version v1), dashed lines without (v0); blue color corresponds to $g_5 = 2\pi$ (OPE fit) and red to the reduced value g_5 (F_ρ-fit).

WP prediction, whereas the result for model v1 (OPE fit) is 2.5σ higher.

The main aim of this study is of course the experimentally less well constrained axial-vector meson contribution, which in holographic QCD has been shown to take into account the Melnikov-Vainshtein short-distance constraint [43,44], also away from the chiral limit [46]. The holographic result thus presents an alternative estimate of the combined contribution of axial-vector mesons, for which the WP estimate is $6(6) \times 10^{-11}$, and of short-distance contributions,[10] estimated in the WP as $15(10) \times 10^{-11}$. With errors added linearly, the WP value is at $21(16) \times 10^{-11}$.

It is difficult to estimate errors for any holographic result, but we expect our results for a_μ to be in good shape despite some deviations in its ingredients. The holographic results for axial-vector mesons have turned out to overestimate the masses of f_1 and f_1' by 8–28%, where the models with gluon condensate have the higher deviations. On the other hand, all our models have an equivalent real photon coupling $A(0,0)$ that is 20–28% too large compared to the value derived from L3 data for f_1 and f_1', albeit in good agreement with the estimate of Ref. [34] for $a_1(1260)$. The mixing angles for f_1 and f_1' are poorly predicted, and even worse when the gluon condensate is turned on. However, the prediction for the amplitude $\sqrt{(A^8)^2 + (A^0)^2}$ appears to be fairly robust and only weakly dependent on Ξ_0. A different modeling of the gluon condensate could perhaps lead to better predictions for the mixing with similar overall amplitude. Our summary in Table IV therefore lists the presumably more reliable combined contribution of f_1 and f_1'. Since the contribution to a_μ decreases with increasing axial-vector meson mass by approximately two inverse

[10]In the symmetric high-energy limit, the holographic results for the HLBL scattering amplitude have the correct dependence on Q^2, but reproduce the OPE value only at the level of 81% when $g_5 = 2\pi$, where the asymmetric MV limit is saturated fully [44,46].

TABLE IV. Summary of the results for the different contributions to a_μ in comparison with the White Paper [4] values.

$a_\mu^{\cdots} \times 10^{11}$	v1(OPE fit)	v1(F_ρ-fit)	WP
π^0	66.1	63.4	$62.6^{+3.0}_{-2.5}$
η	19.3	17.6	16.3(1.4)
η'	16.9	14.9	14.5(1.9)
G/η''	0.2	0.2	
$\sum_{PS^*}$	1.6	1.4	
PS poles total	104	97.5	93.8(4.0)
a_1	7.8	7.1	
$f_1 + f_1'$	20.0	17.9	
$\sum_{a_1^*}$	2.2	2.4	
$\sum_{f_1^{(\prime)*}}$	3.6	3.0	
AV + LSDC total	33.7	30.5	21(16)
Total	138	128	115(16.5)

powers while the amplitude A enters quadratically, we expect that the errors in the predictions of both will largely cancel out, so that the holographic results can still be a reasonably good prediction for the axial-vector meson contributions to a_μ. For our favored model v1(F_ρ-fit), the contribution from the ground-state axial-vector mesons is $a_\mu^{a_1+f_1+f_1'} = 25.0 \times 10^{-11}$, about four times the WP estimate. The contribution from $f_1 + f_1'$ is 2.5 times that of a_1, somewhat reduced from the flavor-U(3)-symmetric value of 3 that was assumed in our previous estimates in Ref. [46]. For this contribution, Pauk and Vanderhaeghen [12] have estimated a value of only $6.4(2.0) \times 10^{-11}$, much smaller than our holographic prediction of 17.9×10^{-11}. Besides the differences in $A(0,0)$ and the mass parameters, a crucial difference of the TFF assumed in [12] is that it is obtained from a factorized ansatz that unlike the holographic result does not have the correct asymptotic behavior [42] in the doubly virtual case, where it falls off as $1/Q^4$ instead of $1/Q^2$.

In the holographic models, the excited axial-vector mesons ensure agreement with the longitudinal (Melnikov-Vainshtein) short-distance constraint. This constraint derived from the axial anomaly is satisfied to 100% in the model v1 (OPE fit), and to 89.4% in the case of v1 (F_ρ-fit). The latter should provide a better approximation at large but still physically relevant energy scales, where typically ∼10% of next-to-leading order pQCD corrections apply [56,57].

In the chiral HW1 model and in the U(3)-symmetric massive HW1m model that we have investigated in Refs. [43,46], we have obtained 9.2 and 9.4×10^{-11} from excited axial vectors, where 25% are due to a_1 by U(3) symmetry. The contribution of excited a_1's in our present models are essentially the same as in the HW1m model (up to a slightly different fit value of f_π), but the excited isoscalars remain below the extra factor of 3 expected from U(3) symmetry.[11] Instead, the latter provide only 1.6 and 1.4 times the contributions from excited a_1's in the case of v1 (OPE fit) and v1(F_ρ-fit), respectively.

The total contribution from axial-vector mesons is thus significantly smaller than the estimates we have come up with in the flavor-symmetric case of Ref. [46]: 33.7 and 30.5×10^{-11} for the two choices of g_5 (instead of 40.8 and 38.8×10^{-11} for HW1m and HW1m with reduced g_5, respectively). Comparing this to the combined estimate of axial-vector mesons and short-distance contributions in the WP, $21(16) \times 10^{-11}$, we find values that are about 50% higher, but well within the estimated error.

V. CONCLUSION

In this paper, we have upgraded our previous studies of the HLBL contribution in HW AdS/QCD models to $2+1$ flavors with strange quark mass $m_s > m_u = m_d$ plus a Witten-Veneziano mass for the flavor-singlet degree of freedom generated by interaction terms involving a pseudoscalar glueball with the latter that implement the anomalous Ward identities of the $U(1)_A$ symmetry in the line of Refs. [48,49].

In holographic QCD, the Melnikov-Vainshtein constraint on the HLBL scattering amplitude is naturally satisfied, to the same degree that TFFs satisfy the Brodsky-Lepage and OPE limits. All these are saturated at the level of 100% for the standard value of $g_5 = 2\pi$ in HW1 models.[12] However, because these models do not involve a running coupling in the UV, the UV limits of TFFs are approached too quickly, likely leading to overestimated HLBL contributions to a_μ. Next-to-leading-order gluonic corrections in pQCD suggest a reduction by about 10% at large but still experimentally relevant virtualities. Precisely such a correction is obtained by fitting g_5 such that the decay constant of the ρ meson is matched instead of the OPE result for the vector correlator. In Ref. [54], we have found that this also moves the $N_f = 2$ result of HW AdS/QCD models for the HVP contribution much closer to the dispersive results [19,20].

In Refs. [43,46] we have shown that the MV short-distance constraint is realized by the infinite tower of axial-vector mesons, with the excited axial-vector mesons adding about a third of the contribution from the ground-state axial

[11] In order to approximate the sum of contributions from the infinite tower of axial-vector mesons we have used the observation that in the chiral HW models as well as in the HW1m model the infinite series of contributions can be roughly approximated by a geometric one with $a_{n+1}/a_n \approx 0.6$ for $n > 2$. The full sum can thus be approximated by multiplying the last contribution of a truncated sum by a factor of $1/(1-0.6) = 2.5$. In the case of excited pseudoscalars, which do not contribute to the longitudinal short-distance constraint [46], the contributions drop much more quickly. Our results for those are obtained simply from the sum of the first few modes.

[12] The simpler Hirn-Sanz (HW2) model, which omits the bifundamental scalar X, reaches 62% when f_π and m_ρ are fitted.

vectors in the flavor-symmetric case. A much smaller contribution comes from excited pseudoscalars, which do not contribute to the longitudinal short-distance behavior at leading order.

In our present study with $U(1)_A$ anomaly included, where we have obtained a remarkably accurate fit of the masses of η and η' mesons as well as of their $F_{P\gamma\gamma}(0,0)$ values when including a nonzero gluon condensate that was omitted in [48], we have found a reduction of the ratio 3:1 for the isoscalar:isotriplet contributions of axial-vector mesons to about 2.5:1. For excited mesons (axial vector as well as pseudoscalar), we have obtained an even more pronounced reduction, which reduces our prediction for the a_μ contribution of axial-vector mesons in the U(3)-symmetric case from around 41 and 39×10^{-11} to 33.7 and 30.5×10^{-11} for $g_5(\mathrm{OPE})$ and $g_5(F_\rho\text{-fit})$, respectively. These values are above the estimate of the White Paper [4] for the contribution of (ground-state) axial-vector mesons plus short-distance constraints, but still within the error given there. The pseudoscalar contributions obtained in our model v1(F_ρ-fit) agree completely with the WP results for π^0, η, and η', however this model also has a contribution of 1.6×10^{-11} from excited pseudoscalars, where the tower of η's mixes with a pseudoscalar glueball. The complete contribution from summing pseudoscalar and axial-vector contributions is approximately 128×10^{-11}, which we consider our currently best estimate obtained from AdS/QCD; it thus turns out to be close to (but below) the upper end of the corresponding WP estimate.

ACKNOWLEDGMENTS

We would like to thank Gilberto Colangelo, Martin Hoferichter, Bastian Kubis, Elias Kiritsis, and Pablo Sanchez-Puertas for helpful discussions. J. L. and J. M. have been supported by the Austrian Science Fund FWF, Project No. P33655, and by the FWF doctoral program Particles and Interactions, Project No. W1252-N27.

[1] B. Abi *et al.* (Muon $g-2$ Collaboration), Measurement of the Positive Muon Anomalous Magnetic Moment to 0.46 ppm, Phys. Rev. Lett. **126**, 141801 (2021).
[2] G. W. Bennett *et al.*, Final report of the E821 muon anomalous magnetic moment measurement at BNL, Phys. Rev. D **73**, 072003 (2006).
[3] F. Jegerlehner, The anomalous magnetic moment of the muon, Second edition, Springer Tracts Mod. Phys. **274**, 1 (2017).
[4] T. Aoyama *et al.*, The anomalous magnetic moment of the muon in the Standard Model, Phys. Rep. **887**, 1 (2020).
[5] T. Aoyama, M. Hayakawa, T. Kinoshita, and M. Nio, Complete Tenth-Order QED Contribution to the Muon $g-2$, Phys. Rev. Lett. **109**, 111808 (2012); T. Aoyama, T. Kinoshita, and M. Nio, Revised and improved value of the QED tenth-order electron anomalous magnetic moment, Phys. Rev. D **97**, 036001 (2018); Theory of the anomalous magnetic moment of the electron, Atoms **7**, 28 (2019).
[6] A. Czarnecki, W. J. Marciano, and A. Vainshtein, Refinements in electroweak contributions to the muon anomalous magnetic moment, Phys. Rev. D **67**, 073006 (2003); **73**, 119901(E) (2006).
[7] C. Gnendiger, D. Stöckinger, and H. Stöckinger-Kim, The electroweak contributions to $(g-2)_\mu$ after the Higgs boson mass measurement, Phys. Rev. D **88**, 053005 (2013).
[8] K. Melnikov and A. Vainshtein, Hadronic light-by-light scattering contribution to the muon anomalous magnetic moment revisited, Phys. Rev. D **70**, 113006 (2004).
[9] J. Prades, E. de Rafael, and A. Vainshtein, The hadronic light-by-light scattering contribution to the muon and electron anomalous magnetic moments, Adv. Ser. Dir. High Energy Phys. **20**, 303 (2009).
[10] A. Kurz, T. Liu, P. Marquard, and M. Steinhauser, Hadronic contribution to the muon anomalous magnetic moment to next-to-next-to-leading order, Phys. Lett. B **734**, 144 (2014).
[11] G. Colangelo, M. Hoferichter, A. Nyffeler, M. Passera, and P. Stoffer, Remarks on higher-order hadronic corrections to the muon $g-2$, Phys. Lett. B **735**, 90 (2014).
[12] V. Pauk and M. Vanderhaeghen, Single meson contributions to the muon's anomalous magnetic moment, Eur. Phys. J. C **74**, 3008 (2014).
[13] M. Davier, A. Hoecker, B. Malaescu, and Z. Zhang, Reevaluation of the hadronic vacuum polarisation contributions to the Standard Model predictions of the muon $g-2$ and $\alpha(m_Z^2)$ using newest hadronic cross-section data, Eur. Phys. J. C **77**, 827 (2017).
[14] P. Masjuan and P. Sanchez-Puertas, Pseudoscalar-pole contribution to the $(g_\mu-2)$: A rational approach, Phys. Rev. D **95**, 054026 (2017).
[15] G. Colangelo, M. Hoferichter, M. Procura, and P. Stoffer, Dispersion relation for hadronic light-by-light scattering: Two-pion contributions, J. High Energy Phys. 04 (2017) 161.
[16] A. Keshavarzi, D. Nomura, and T. Teubner, Muon $g-2$ and $\alpha(M_Z^2)$: A new data-based analysis, Phys. Rev. D **97**, 114025 (2018).
[17] G. Colangelo, M. Hoferichter, and P. Stoffer, Two-pion contribution to hadronic vacuum polarization, J. High Energy Phys. 02 (2019) 006.
[18] M. Hoferichter, B.-L. Hoid, and B. Kubis, Three-pion contribution to hadronic vacuum polarization, J. High Energy Phys. 08 (2019) 137.
[19] M. Davier, A. Hoecker, B. Malaescu, and Z. Zhang, A new evaluation of the hadronic vacuum polarisation contributions

to the muon anomalous magnetic moment and to $\alpha(m_Z^2)$, Eur. Phys. J. C **80**, 241 (2020).
[20] A. Keshavarzi, D. Nomura, and T. Teubner, $g-2$ of charged leptons, $\alpha(M_Z^2)$, and the hyperfine splitting of muonium, Phys. Rev. D **101**, 014029 (2020).
[21] M. Hoferichter, B.-L. Hoid, B. Kubis, S. Leupold, and S. P. Schneider, Pion-Pole Contribution to Hadronic Light-by-Light Scattering in the Anomalous Magnetic Moment of the Muon, Phys. Rev. Lett. **121**, 112002 (2018); Dispersion relation for hadronic light-by-light scattering: Pion pole, J. High Energy Phys. 10 (**2018**) 141.
[22] A. Gérardin, H. B. Meyer, and A. Nyffeler, Lattice calculation of the pion transition form factor with $N_f = 2+1$ Wilson quarks, Phys. Rev. D **100**, 034520 (2019).
[23] J. Bijnens, N. Hermansson-Truedsson, and A. Rodríguez-Sánchez, Short-distance constraints for the HLbL contribution to the muon anomalous magnetic moment, Phys. Lett. B **798**, 134994 (2019).
[24] J. Bijnens, N. Hermansson-Truedsson, L. Laub, and A. Rodríguez-Sánchez, Short-distance HLbL contributions to the muon anomalous magnetic moment beyond perturbation theory, J. High Energy Phys. 10 (2020) 203.
[25] G. Colangelo, F. Hagelstein, M. Hoferichter, L. Laub, and P. Stoffer, Short-distance constraints on hadronic light-by-light scattering in the anomalous magnetic moment of the muon, Phys. Rev. D **101**, 051501 (2020).
[26] G. Colangelo, F. Hagelstein, M. Hoferichter, L. Laub, and P. Stoffer, Longitudinal short-distance constraints for the hadronic light-by-light contribution to $(g-2)_\mu$ with large-N_c Regge models, J. High Energy Phys. 03 (2020) 101.
[27] I. Danilkin, C. F. Redmer, and M. Vanderhaeghen, The hadronic light-by-light contribution to the muon's anomalous magnetic moment, Prog. Part. Nucl. Phys. **107**, 20 (2019).
[28] T. Blum, N. Christ, M. Hayakawa, T. Izubuchi, L. Jin, C. Jung, and C. Lehner, Hadronic Light-by-Light Scattering Contribution to the Muon Anomalous Magnetic Moment from Lattice QCD, Phys. Rev. Lett. **124**, 132002 (2020).
[29] E.-H. Chao, R. J. Hudspith, A. Gérardin, J. R. Green, H. B. Meyer, and K. Ottnad, Hadronic light-by-light contribution to $(g-2)_\mu$ from lattice QCD: A complete calculation, Eur. Phys. J. C **81**, 651 (2021).
[30] M. Hoferichter and T. Teubner, Mixed Leptonic and Hadronic Corrections to the Anomalous Magnetic Moment of the Muon, Phys. Rev. Lett. **128**, 112002 (2022).
[31] I. Danilkin, M. Hoferichter, and P. Stoffer, A dispersive estimate of scalar contributions to hadronic light-by-light scattering, Phys. Lett. B **820**, 136502 (2021).
[32] S. Borsanyi *et al.*, Leading hadronic contribution to the muon magnetic moment from lattice QCD, Nature (London) **593**, 51 (2021).
[33] J. Bijnens, E. Pallante, and J. Prades, Comment on the pion pole part of the light by light contribution to the muon $g-2$, Nucl. Phys. **B626**, 410 (2002).
[34] P. Roig and P. Sanchez-Puertas, Axial-vector exchange contribution to the hadronic light-by-light piece of the muon anomalous magnetic moment, Phys. Rev. D **101**, 074019 (2020).
[35] P. Masjuan, P. Roig, and P. Sanchez-Puertas, The interplay of transverse degrees of freedom and axial-vector mesons with short-distance constraints in $g-2$, J. Phys. G **49**, 015002 (2022).
[36] J. M. Maldacena, The large N limit of superconformal field theories and supergravity, Int. J. Theor. Phys. **38**, 1113 (1999).
[37] E. Witten, Anti-de Sitter space, thermal phase transition, and confinement in gauge theories, Adv. Theor. Math. Phys. **2**, 505 (1998).
[38] O. Aharony, S. S. Gubser, J. M. Maldacena, H. Ooguri, and Y. Oz, Large N field theories, string theory and gravity, Phys. Rep. **323**, 183 (2000).
[39] J. Leutgeb, J. Mager, and A. Rebhan, Pseudoscalar transition form factors and the hadronic light-by-light contribution to the anomalous magnetic moment of the muon from holographic QCD, Phys. Rev. D **100**, 094038 (2019); **104**, 059903(E) (2021).
[40] D. K. Hong and D. Kim, Pseudo scalar contributions to light-by-light correction of muon $g-2$ in AdS/QCD, Phys. Lett. B **680**, 480 (2009).
[41] L. Cappiello, O. Cata, and G. D'Ambrosio, The hadronic light by light contribution to the $(g-2)_\mu$ with holographic models of QCD, Phys. Rev. D **83**, 093006 (2011).
[42] M. Hoferichter and P. Stoffer, Asymptotic behavior of meson transition form factors, J. High Energy Phys. 05 (2020) 159.
[43] J. Leutgeb and A. Rebhan, Axial vector transition form factors in holographic QCD and their contribution to the anomalous magnetic moment of the muon, Phys. Rev. D **101**, 114015 (2020).
[44] L. Cappiello, O. Catà, G. D'Ambrosio, D. Greynat, and A. Iyer, Axial-vector and pseudoscalar mesons in the hadronic light-by-light contribution to the muon $(g-2)$, Phys. Rev. D **102**, 016009 (2020).
[45] G. Colangelo, F. Hagelstein, M. Hoferichter, L. Laub, and P. Stoffer, Short-distance constraints for the longitudinal component of the hadronic light-by-light amplitude: An update, Eur. Phys. J. C **81**, 702 (2021).
[46] J. Leutgeb and A. Rebhan, Hadronic light-by-light contribution to the muon $g-2$ from holographic QCD with massive pions, Phys. Rev. D **104**, 094017 (2021).
[47] J. Erlich, E. Katz, D. T. Son, and M. A. Stephanov, QCD and a Holographic Model of Hadrons, Phys. Rev. Lett. **95**, 261602 (2005).
[48] E. Katz and M. D. Schwartz, An eta primer: Solving the U(1) problem with AdS/QCD, J. High Energy Phys. 08 (2007) 077.
[49] T. Schäfer, Euclidean correlation functions in a holographic model of QCD, Phys. Rev. D **77**, 126010 (2008).
[50] L. Da Rold and A. Pomarol, Chiral symmetry breaking from five-dimensional spaces, Nucl. Phys. **B721**, 79 (2005).
[51] H. R. Grigoryan and A. V. Radyushkin, Pion form-factor in chiral limit of hard-wall AdS/QCD model, Phys. Rev. D **76**, 115007 (2007).
[52] Z. Abidin and C. E. Carlson, Strange hadrons and kaon-to-pion transition form factors from holography, Phys. Rev. D **80**, 115010 (2009).

[53] O. Domènech, G. Panico, and A. Wulzer, Massive pions, anomalies and baryons in holographic QCD, Nucl. Phys. **A853**, 97 (2011).
[54] J. Leutgeb, A. Rebhan, and M. Stadlbauer, Hadronic vacuum polarization contribution to the muon $g-2$ in holographic QCD, Phys. Rev. D **105**, 094032 (2022).
[55] M. A. Shifman, A. I. Vainshtein, and V. I. Zakharov, QCD and resonance physics. Theoretical foundations, Nucl. Phys. **B147**, 385 (1979).
[56] B. Melic, D. Mueller, and K. Passek-Kumericki, Next-to-next-to-leading prediction for the photon to pion transition form-factor, Phys. Rev. D **68**, 014013 (2003).
[57] J. Bijnens, N. Hermansson-Truedsson, L. Laub, and A. Rodríguez-Sánchez, The two-loop perturbative correction to the $(g-2)_\mu$ HLbL at short distances, J. High Energy Phys. 04 (2021) 240.
[58] L. Cappiello, O. Catà, and G. D'Ambrosio, Scalar resonances in the hadronic light-by-light contribution to the muon $(g-2)$, Phys. Rev. D **105**, 056020 (2022).
[59] V. Pascalutsa, V. Pauk, and M. Vanderhaeghen, Light-by-light scattering sum rules constraining meson transition form factors, Phys. Rev. D **85**, 116001 (2012).
[60] M. Zanke, M. Hoferichter, and B. Kubis, On the transition form factors of the axial-vector resonance $f_1(1285)$ and its decay into e^+e^-, J. High Energy Phys. 07 (2021) 106.
[61] Y. Aoki *et al.* (Flavour Lattice Averaging Group (FLAG)), FLAG review 2021, Eur. Phys. J. C **82**, 869 (2022).
[62] F. Brünner and A. Rebhan, Constraints on the $\eta\eta'$ decay rate of a scalar glueball from gauge/gravity duality, Phys. Rev. D **92**, 121902 (2015).
[63] R. Escribano and J.-M. Frère, Phenomenological evidence for the energy dependence of the η-η' mixing angle, Phys. Lett. B **459**, 288 (1999).
[64] R. Escribano and J.-M. Frère, Study of the η-η' system in the two mixing angle scheme, J. High Energy Phys. 06 (2005) 029.
[65] G. S. Bali, V. Braun, S. Collins, A. Schäfer, and J. Simeth (RQCD Collaboration), Masses and decay constants of the η and η' mesons from lattice QCD, J. High Energy Phys. 08 (2021) 137.
[66] R. L. Workman *et al.* (Particle Data Group), Review of particle physics, Prog. Theor. Exp. Phys. **2022**, 083C01 (2022).
[67] P. Achard *et al.* (L3 Collaboration), $f_1(1285)$ formation in two-photon collisions at LEP, Phys. Lett. B **526**, 269 (2002).
[68] L3 Collaboration, Study of resonance formation in the mass region 1400–1500 MeV through the reaction $\gamma\gamma \to K^0_S K^\pm \pi^\mp$, J. High Energy Phys. 03 (2007) 018.
[69] R. Casero, E. Kiritsis, and A. Paredes, Chiral symmetry breaking as open string tachyon condensation, Nucl. Phys. **B787**, 98 (2007).
[70] D. Areán, I. Iatrakis, M. Järvinen, and E. Kiritsis, The discontinuities of conformal transitions and mass spectra of V-QCD, J. High Energy Phys. 11 (2013) 068.
[71] F. Giannuzzi and S. Nicotri, $U(1)_A$ axial anomaly, η', and topological susceptibility in the holographic soft-wall model, Phys. Rev. D **104**, 014021 (2021).
[72] J. P. Lees *et al.* (*BABAR* Collaboration), Measurement of the $\gamma^*\gamma^* \to \eta'$ transition form factor, Phys. Rev. D **98**, 112002 (2018).